

**Current microscopy contributions to advances in  
science and technology**

FORMATEX  
Microscopy Series N° 5

VOL. 2

**Edited by**

A. Méndez-Vilas

ISBN-13 Vol. 2: 978-84-939843-6-6  
ISBN-13 Collection: 978-84-939843-4-2

Formatex Research Center  
C/ Zurbarán 1, 2º - Oficina 1  
06002 Badajoz  
Spain  
<http://www.formatex.org>

Printed in Spain

## TABLE OF CONTENTS

### VOL. 1

<b>Introduction</b> .....	xv
<b>Applications in Biology and Medicine</b>	
<b>Analysis of fluorescent nanostructures in biological systems by means of Spectral Position Determination Microscopy (SPDM)</b>	
Patrick Müller, Yanina Weiland, Rainer Kaufmann, Manuel Gunkel, Sabina Hillebrandt, Christoph Cremer, Michael Hausmann.....	3-12
<b>Autofocus functions for tuberculosis diagnosis with conventional sputum smear microscopy</b>	
C. F. Fernandes Costa Filho, M. G. Fernandes Costa and A. Kimura Júnior.....	13-20
<b>Microscopic anatomy of aquatic oligochaetes (Annelida, Clitellata): a zoological perspective</b>	
Carlos Caramelo and Enrique Martínez-Ansemil.....	21-27
<b>Picrosirius Staining for Dystrophic Animal Models of Diaphragm Morphology</b>	
D. Kelly de Abreu, T. Borges Lessa, B. Machado Bertassoli, H. Debiazi Zomer, P. Fratini, S. Elisabete Alves de Lima Will, R. Eli Grassi Rici, R. Agostinho da Silva, A. C. Assis Neto, M. Angélica Miglino and C.E. Ambrósio.....	28-32
<b>The applications of NSOM/QDs-based single-molecule in situ detection on cell membrane</b>	
Jiang Pi, and Jiye Cai.....	33-45
<b>The usefulness of bone marrow in the standardization process of immunohistochemical methods</b>	
Marta Ortega-Martínez, Alberto Niderhauser-García, Edgar Romero-Núñez, Ivett C. Miranda-Maldonado, Carlos de la Garza-González, Jesús Ancer-Rodríguez and Gilberto Jaramillo-Rangel.....	46-51
<b>Application of advanced confocal microscopic observation in animal reproductive medicine</b>	
Bartosz Kempisty, Agnieszka Ziółkowska, Hanna Piotrowska, Piotr Zawierucha, Paweł Antosik, Dorota Bukowska, Jędrzej M. Jaśkowski, Michał Nowicki, Klaus P. Brüssow, Maciej Zabel.....	52-61
<b>Applications of confocal microscopy to the study of vascular biology</b>	
C. B. A. Restini and L.M. Bendhack.....	62-75
<b>Confocal imaging of organotypic brain slices for real time analysis of cell death</b>	
A. Merighi, S. Alasia, G. Gambino, and L. Lossi.....	76-83
<b>Confocal microscopy and spectral imaging technique: contribution to the development of neutron sensitizers for anticancer BNCT</b>	
A.V. Efremenko, A.A. Ignatova, M.A. Grin, A.F. Mironov, V.I. Bregadze, I.B. Sivaev and A.V. Feofanov.....	84-90
<b>Structural characteristics of <i>in situ</i> undisturbed human oral biofilm and activity of antimicrobial agents</b>	
I. Tomás, L. García-Caballero and J.M. Seoane.....	91-102
<b>Label-free microscopy: spectral imaging of multiphoton-excited cellular autofluorescence</b>	
A. Holloschi, HM. Kuhn, C. Müller, M. Worf, M. Rauen, T. Röder, W. Kessler, J. Mollenhauer and P. Kioschis.....	103-111
<b>Molecular similarities between spermatozoa and bacteria: A fluorescent microscopy study</b>	
Vijay Prabha and Harpreet Vander.....	112-118

<b>Quantitative Imaging of Intracellular Sodium</b> A. E. Schreiner and C. R. Rose.....	119-129
<b>Standardization and quantification of fluorescent probes in epifluorescence microscopy</b> Martyn A. Sharpe PhD, Andrew D. Livingston MD, Leonardo Rangel-Castilla MD, and David S. Baskin MD.....	130-139
<b>Study of EphA2 dimerization and clusterization in living cells using sensitized acceptor emission in FRET pair</b> G.V. Sharonov, M.N. Mozgovaja, M.V. Astapova, P.M. Kolosov, A.S. Arseniev and A.V. Feofanov....	140-147
<b>A new approach for three-dimensional visualization of cryostat sections</b> Eleonora Franzetti, Terenzio Congiu, Petra Basso, Magda de Eguileor, Gianluca Tettamanti.....	148-153
<b>Biological nanostructures associated to iberulites: a SEM study</b> J.L. Díaz-Hernández, P.J. Sánchez-Soto and A. Serrano-Delgado.....	154-161
<b>Dystrophic animal models of diaphragm morphology for muscle ultrastructural analysis</b> T. Borges Lessa; B. Machado Bertassoli; S. Elisabete Alves de Lima Will; M. Pandolphi Brólio; D. Kelly de Abreu; R. Eli Grassi Rici; M. Angelica Miglino and Carlos E. Ambrósio.....	162-166
<b>Electron microscopy and immunogold labelling analysis of smart nanoparticles (storage proteins) in insects</b> Chandrasekar Raman .....	167-178
<b>FIB/SEM/EDS complementary analysis for proper forensic interpretation</b> M. Milani, R. Gottardi, C. Savoia and C. Cattaneo.....	179-185
<b>Microscopic imaging of the endometrium for assessment of uterine receptivity in women with latent genital tuberculosis</b> Elavarasan Subramani, Priyanka Banerjee, Chaitali Dattaray, Debashis Chakrabarty, Baidyanath Chakravarty and Koel Chaudhury.....	186-190
<b>Morphometric SEM 3D analysis of microvascular networks and automated calculation of vessel angioarchitecture optimalities</b> B. Minnich, S. Margiol, J. Fryszak and E.W.N. Bernroider.....	191-199
<b>Osteosarcoma treatment using the different bone growth factors</b> D. Alcântara, S. E. A. L. Will, P. Fratini, A. L. R. Francioli, R. E. G. Rici, D. K. Abreu, R. M. Leandro, F. M. O. Silva, M. N. Rodrigues and M. A. Miglino.....	200-206
<b>Parasitic fungi on roses</b> Marcel Pârvu, Alina E. Pârvu.....	207-214
<b>Pros and cons of scanning electron microscopy as a research method in acarology</b> Zbigniew Adamski, Eliza Rybska and Jerzy Błoszyk .....	215-221
<b>Scanning Electron Microscopy coupled to an Energy Dispersive X-ray detector to study copper removal on different phototrophic microorganisms</b> Álvaro Burgos, Marina Seder-Colomina, Juan Maldonado, Antonio Solé and Isabel Esteve.....	222-229
<b>Scanning electron microscopy detection of seed-borne fungi in blotter test</b> Marcelo de Carvalho Alves and Edson Ampélio Pozza.....	230-238
<b>Scanning Electron Microscopy of vascular corrosion cast – a bench-to-bedside approach in cancer research</b> V. Faccin Bampi, J. Rangel Oliveira, S.M. Encarnação Fiala Rechsteiner, M.G. Tavares Rheingantz, L.F. Minello, J.L. Braga da Silva, L.B. Oliveira de Oliveira.....	239-244

<b>Techniques Used for Morphological and Ultrastructural Description from Teeth White-Tufted-Ear-Marmosets (<i>Callithrix jacchus</i>)</b> B. Machado Bertassoli, T. Borges Lessa, F. Delys de Oliveira, D. Kelly de Abreu, L. C. Stunitz da Silva, A. Cesar dos Santos, R. Eli Grassi Rici, A. C. Assis Neto.....	245-250
<b>A “non-classical” and reliable method for transmission immunoelectron microscopy.</b> P. Lenzi, M. Ferrucci, G. Lazzeri, F. Fulceri, F. Fornai and A. Falleni.....	251-258
<b>Applications of Transmission Electron Microscopy to evaluate the diversity of the male reproductive system of Neotropical bats</b> M. R. Beguelini, C. C. I. Puga, F. F. Martins, A. C. Negrin, C. M Christante, P. S. L. Vilamaior, S. R. Taboga and E. Morielle-Versute.....	259-268
<b>Correlation between granulocytes and tunic cuticle of <i>Ciona intestinalis</i> (Tunicata, Ascidiacea) as evaluated by microscopy</b> M. A. Di Bella and G. De Leo.....	269-272
<b>Electron microscopy and immunogold labelling of proteins involved in brain tumour growth and invasion</b> J.A. Miyake and A. Colquhoun.....	273-279
<b>Microcalcifications as seen in epoxy-embedded carotids using a trichromic staining</b> M. Relucenti, L. Petruzzello, R. Heyn , E. Battaglione and G. Familiari.....	280-285
<b>Microscopic features of mitochondria rejuvenation by amino acids</b> A. Stacchiotti , G. Corsetti , A.Lavazza and R.Rezzani.....	286-294
<b>The effect of hypertriglyceridemia on the integrity of endothelial monolayer structure of rat aorta: electron microscopic and immunofluorescent analysis</b> Ľ.Okruhlicová, K.Frimmel, P.Weismann, J.Slezák.....	295-301
<b>Ultrastructural cytoplasmic characteristics of domestic cat (<i>Felis catus</i>) oocytes according to ovarian status and <i>in vitro</i> maturation</b> Lilian Rigatto Martins, Rayf Roberto Tirloni, Fernanda da Cruz Landim-Alvarenga and Maria Denise Lopes.....	302-308
<b>Ultrastructural morphometric analysis by transmission electron microscopy associated with stereology methods</b> N. Nathaly Rigoglio, M. V. Mendes Silva, V. Pavanelo Junior, S. A. Ferreira Lima, J. Luiz Nogueira, R. Avancini Fernandes and M. A. Miglino.....	309-315
<b>Use of PEG, Polyethylene glycol, to characterize the diversity of environmental viruses</b> Jonathan Colombet and Téséphore Sime-Ngando.....	316-322
<b>Biodestruction of polyurethane by <i>Staphylococcus aureus</i> (an investigation by SEM, TEM and FIB )</b> Didenko L.V., Avtandilov G.A., Shevlyagina N.V., Smirnova T.A., Lebedenko I.Y., Tatti F., Savoia C., Evans G. and Milani M.....	323-334
<b>Electron microscopy and the responses of terrestrial invertebrates against contaminants of soil</b> C. S. Fontanetti, T. G. Pinheiro, R. B. Souza, A. C. de C. Marcato and C. Moreira de Sousa.....	335-342
<b>Electron microscopy in the study of human sperm pathologies</b> E. Moretti and G. Collodel.....	343-351
<b>Morphological description of the placenta in armadillo (<i>Chaetophractus vellerosus</i> and <i>Euphractus sexcinctus</i>)</b> L. C. Rezende, S. A. S. Kückelhaus, C. Barbeito, and J. R. Ferreira.....	352-357

<b>Quantification of immunogold labelling in two populations of dendritic cells: a study on endogenous protease inhibitor</b> T. Zavašnik-Bergant.....	358-365
<b>Role of Electron Microscopy-Immunocytochemistry and In Situ Hybridization in the Study of Oxidative Stress-Induced Mitochondrial Abnormalities and the Pathobiology of Neurodegeneration and Cancer</b> Gjumrakch Aliev, V. Prakash Reddy and Ramon Cacabelos.....	366-385
<b>The importance of electron microscopy and a study of type IV collagen alpha chains in the diagnosis of Thin Basement Membrane Glomerulopathy and Alport Syndrome</b> Juliana Reis Machado, Valéria Lima laterza, Vanessa Fraga Mendes, Crislaine Aparecida da Silva, Maria Laura Pinto, Marcos vinícius da Silva, Ana carolina Guimarães Faleiros and Marlene Antônia dos Reis.....	386-393
<b>Ultrastructural evidences of the plastron organization and skin respiration in the soil inhabiting trombiculid mites (Acariformes: Trombiculidae)</b> Andrew B. Shatrov.....	394-400
<b>Use of scanning and transmission electron microscopy to identify morphological and cellular damage on phytopathogenic fungi due to natural products application</b> S. Bautista-Baños, M. de L. Ramos-García, M. Hernández-López, L. Córdova-Albores, L. I. López-Mora, P. Gutiérrez-Martínez and D. Sánchez-Domínguez.....	401-405
<b>Microscopic assessment of scaffold ultrastructure for tissue engineering applications</b> Costantino Del Gaudio, Silvia Baiguera, Paolo Macchiarini, and Alessandra Bianco.....	406-413
<b>Microscopical study of the digestive tract of Blue and Yellow macaws</b> M. N. Rodrigues, J. A. P. Abreu, C. Tivane, P. G. Wagner, D. B. Campos, R. R. Guerra, R. E. G. Ricci and M. A. Miglino.....	414-421
<b>Structure of elastic-fiber microfibrils more dynamic than that in non-elastic tissue</b> T. Sawada and S. Inoue.....	422-428
<b>Evaluation of the efficiency of two fasteners used in the preservation of the testicular parenchyma</b> P. R. Silva Santos; P. A. Cardoso Luz; C. Andrighetto and A. C. Assis Neto.....	429-432
<b>Immunohistochemical markers to differentiate oral precancerous and cancerous lesion: an integrated tissue-based microscopic analysis</b> Sanjit Mukherjee, Atul Katarkar, Jay Gopal Ray and Keya Chaudhuri.....	433-438
<b>The hydrophilie of the larval test of Ascidia: functional role played by test cells</b> G. Dolcemascolo, M. A. Di Bella and M. Gianguzza.....	439-444
<b>Dynamic Microscopy: Reconstructing a Novel Lysosomal Trafficking Pathway</b> Libin Yuan, Flavia Lorena Carvelli and Carlos R. Morales.....	445-457
<b>Immunostaining of Glycosaminoglycans and Proteoglycans in Marine Organisms</b> C. Monteiro de Barros, M. S. Gonçalves Pavão and S. Allodi.....	458-470
<b>Light and electron microscopy applied to the characterization of marine species belonging to the genus <i>Chloromyxum</i>, as a study model for myxosporean parasites</b> S. Rocha and C. Azevedo.....	471-477
<b>Live CLEM imaging: an application for yeast cells</b> Haruhiko Asakawa, Yasushi Hiraoka, and Tokuko Haraguchi.....	478-485

<b>Meat and meat products microstructure and their eating quality</b> Massami Shimokomaki, Elza I. Ida, Talita Kato, Mayka R. Pedrão, Fabio A. G. Coró and Francisco J. Hernández-Blazquez.....	486-495
<b>Studies on Blood-Brain Barrier and Brain Edema in Central Nervous System Injury Using Light and Electron Microscopy</b> Aruna Sharma, Dafin F. Muresanu, Herbert Mössler and Hari S. Sharma.....	496-507
<b>The structure of the bovine yolk sac: a study microscopic</b> A. C. Galdos-Riveros, L. C. Rezende, A. G. T. Pessolato, M. A. Zogno, R. E. Rici and M. A. Miglino...	508-515
<b>Use of Microscopy to Investigate Nanoparticles Induced Neurotoxicity and Neurorepair Following Nanodrug Delivery</b> Hari S. Sharma, José V. Lafuente, Z. Ryan Tian and Aruna Sharma.....	516-527
<b>Atomic force microscopy: Studying mechanical properties of a cell</b> J. Malohlava, H. Zapletalova, K. Tomankova and H. Kolarova.....	528-532
<b>Characterization of the structural/properties correlation of crosslinked dentin collagen fibrils: AFM study</b> Amr S Fawzy, Lu Thong Beng and NgMah-Lee.....	533-539
<b>Imaging of Cells, Viruses, and Virus - Infected Cells by Atomic Force Microscopy</b> A. McPherson and Yu. G. Kuznetsov.....	540-548
<b>Mechanical Characterisation of HeLa Cells using Atomic Force Microscopy</b> K. Tomankova, P. Kolar, J. Malohlava and H. Kolarova.....	549-554
<b>Study of developmental enamel defects of permanent teeth by atomic force microscopy</b> E. Kaplova, K. Tomankova, H. Kolarova, P. Krejci.....	555-560
<b>The study of living and fixing buccal epitheliocytes morphology by atomic force microscopy</b> E. Lesniewska, E. Bourillot, D. Carriou, J. Gushina, E. Pudovkina and S.N. Pleskova.....	561-568
<b>Applications of Confocal Laser Scanning Microscopy in Dentistry. Study of the changes of the post-extraction sites</b> Ariadna García-Herraiz, Rafael Leiva-García, Francisco Javier Silvestre and José García-Antón.....	569-581
<b>Superradiant rare-earth doped nanocrystals in the study of persorption processes in the adult intestine</b> M. M. Godlewski and M. Godlewski.....	582-590
<b>Current opinion in tissue engineering microscopy techniques</b> L. Tayebi , A. Nozari , D. Vashae and M. Mozafari.....	591-601
<b>The use of the light microscopy and the atomic force microscopy for studying cell death under hydrogen peroxide influence</b> Svetlana Pleskova.....	602-609
<b>Microscopic aspects of the yolk sac hematopoiesis from ovine embryos</b> A. G. T. Pessolato, D. S. Martins, A. Galdos-Riveros, A. M. Fontes, C. E. Ambrósio, R. E. Grassi Rici, D. A. R. Magalhães, A. Castilho-Fernandes, D. T. Covas and M. A. Miglino.....	610-616
<b>Interaction of HPV16L1L2 VLP with stem cells CD34<sup>+</sup>/CD117<sup>+</sup> of the human amniotic fluid</b> E.A. Kavati, A.C.M. Palumbo, F.B. Andrade, B. Marigliani, D. Sakauchi, E. Leão, E. Armbruster-Moraes, M. Müller, and A.M. Cianciarullo.....	617-624
<b>Microscopic methods to study the structure of scaffolds in bone tissue engineering: a brief review</b> Mazeyar Parvinzadeh Gashti, Farbod Alimohammadi, Jürg Hulliger, Matthias Burgener, Hanane Oulevey-Aboulfad and Gary L. Bowlin.....	625-638

<b>Microscopy as a tool to follow deconstruction of lignocellulosic biomass</b> Celso Sant'Anna and Wanderley de Souza.....	639-645
<b>Microscopy in mycological research with especial reference to ultrastructures and biofilm studies</b> Iqbal Ahmad and Mohd Sajjad Ahmad Khan.....	646-659
<b>Contribution of electron microscopy and atomic force microscopy to investigate the unique organization of mitochondrial DNA from trypanosomatid protozoa</b> Danielle Pereira Cavalcanti and Wanderley de Souza.....	660-667
<b>Probing dynamic fibril-formation by an integrated microscopic approach</b> Y. Cao, D. Hamada, Y. Kong, P. Cao, J. Guo and J. Chen.....	668-677
<b>Intracellular distribution of recombinant Human Papillomavirus capsid proteins</b> B. Marigliani, E.A. Kavati, D. Sakauchi, H. B. Oliveira, R. A. Canali, A. A. Sasaki, J. M. C. Ferreira Jr, E. Armbruster-Moraes, M. Müller and A.M. Cianciarullo.....	678-684
<b>Integrated Optical Systems for Laser Nanosurgery and Optical Trapping to Study Cell Structure and Function</b> L. Z. Shi, Q. Zhu, T. Wu, M. L. Duquette, V. Gomez, C. Chandsawangbhuwana, M. S. Harsono, N. Hyun, N. Baker, J. Nascimento, Z. You, E. B. Botvinick and M. W. Berns.....	685-695
<b>Protocol for optimization of histological, histochemical and immunohistochemical analyses of larval tissues: application in histopathology of honey bee</b> E. C. M. Silva-Zacarin, M. P. Chauzat, S. Zeggane, P. Drajnudel, F. Schurr, J. P. Faucon, O. Malaspina, J. A. Engler.....	696-703
<b>The usage of microscopy method for herbal standardizations</b> Subramanion Jothy Lachumy and Sreenivasan Sasidharan.....	704-710
<b>Comparative analysis of female gonad characters in neophoran Platyhelminthes: an ultrastructural and cytochemical overview</b> A. Falleni, P. Lucchesi and C. Ghezzani.....	711-722
<b>Microscopical features of the digestive tract in the rhea (<i>Rhea Americana americana</i>, Linnaeus, 1758)</b> M. N. Rodrigues, G. B. Oliveira, R. S. B. Silva, C. Tivane, J. F. G. Albuquerque, M. A. Miglino and M. F. Oliveira.....	723-728
<b>Application of the digital holographic interference microscopy for study of 3D morphology of human blood erythrocytes</b> T.V. Tishko, D.N. Tishko and V. P. Titar.....	729-736
<b>Stereological methods for quantitative assessment of hepatic microcirculation</b> Z. Tonar, L. Eberlová, J. Polívka, O. Daum, K. Witter, A. Králíčková, T. Gregor, L. Nedorost, P. Kochová, E. Rohan, K. Kalusová, R. Pálek, M. Skála, D. Glanc, M. Králíčková and V. Liška.....	737-748
<b>Metallurgical microscopy of Bacterial biofilm representing Cr<sup>+6</sup> conversion into Cr<sup>+3</sup> by <i>Acinetobacter calcoaceticus</i>, <i>Staphylococcus aureus</i> and <i>Oscillatoria strain</i>.</b> Anjum Nasim Sabri, Sabeen Sabri and Sikander Sultan.....	749-755
<b>Cell morphological changes combined with biochemical assays for assessment of apoptosis and apoptosis reversal.</b> Chaitanya Joshi, Bharat Karumuri, Jamie J. Newman and Mark A. DeCoster.....	756-762
<b>Molecular Characterisation of Cell-penetrating Peptides through Live Cell Microscopy – the Past, the Present and the Future</b> Anthony Jin Shun CHUA, Patricia Annabelle NETTO, and Mah Lee NG.....	763-774



<b>Robotic Microscopy and information technology to increase accuracy, sensitivity and availability of blood cell analyses</b> V. Medovyi and A. Pyatnitskiy.....	775-781
--	---------

<b>Applications of micro-computed tomography in endodontic research</b> M.A. Marciano, M.A.H. Duarte, R. Ordinola-Zapata, A. Del Carpio Perochena, B.C. Cavenago, M.H. Villas-Bôas, P.G. Minotti, C.M. Bramante and I.G. Moraes.....	782-788
--	---------

## VOL. 2

<b>Introduction</b> .....	xv
---------------------------	----

### Advances in Instrumentation and Techniques

<b>Building a fast scanning stimulated emission depletion microscope: a step by step guide</b> Pedro Felipe Gardeazábal Rodríguez, Yong Wu, Harpreet Singh, Hui Zhao, Ligia Toro and Enrico Stefani.....	791-800
--	---------

<b>Optical characterization of subwavelength apertures</b> N.I. Petrov.....	801-808
--	---------

<b>The White Confocal – Spectral Gaps Closed</b> R. T. Borlinghaus and L. R. Kuschel.....	809-817
--	---------

<b>Detectors for Sensitive Detection: HyD</b> R. T. Borlinghaus, H. Birk and F. Schreiber.....	818-825
---	---------

<b>Current optical sectioning systems in florescence microscopy</b> Pavel Křížek and Guy M. Hagen.....	826-832
---	---------

<b>Immobilization of living specimens for microscopic observation</b> Karl J. Aufderheide and Christopher Janetopoulos.....	833-837
--	---------

<b>Light Sheet Fluorescence Microscopy: beyond the flatlands</b> Gutiérrez-Heredia Luis, Flood Peter. M., and Emmanuel G. Reynaud.....	838-847
---	---------

<b>STED and GSDIM: Diffraction Unlimited Resolution for all Types of Fluorescence Imaging</b> R. T. Borlinghaus.....	848-854
---	---------

<b>Characterization of food texture: application of Microscopic technology</b> M. Fazaeli, M. Tahmasebi and Z. Emam.Djomeh.....	855-871
--	---------

<b>Tissue and cytoplasm vitrification in cryopreservation monitored by low temperature scanning electron microscopy (cryo-SEM)</b> A.S. Teixeira, M.E. González -Benito and A.D. Molina-García.....	872-879
--	---------

<b>Practical Considerations in the Successful Preparation of Specimens for Thin-Film Cryo-Transmission Electron Microscopy</b> D. Cheng, D.R.G. Mitchell, D-B. Shieh, F. Braet.....	880-890
--	---------

<b>Electron Microscopy in the Perspective of Modern Biology: Ultravision and Ultradimension</b> Somnath Chatterjee, Anirban Roy , Aparna Laskar and Snehasikta Swarnakar.....	891-902
--	---------

<b>Quantitative image analysis of food microstructure</b> G. Impoco, N. Fucà, L. Tuminello and G. Licitra.....	903-911
---	---------

<b>Cryo-TEM and AFM for the characterization of vesicle-like nanoparticle dispersions and self-assembled supramolecular fatty-acid-based structures: a few examples.</b> Cédric Gaillard and Jean-Paul Douliez.....	912-922
<b>Scale laws for AFM image evaluation: potentialities and applications</b> M. Prado, L. C. Lima and R. A. Simão.....	923-929
<b>Scanning Tunnelling Microscopy: a powerful probe of unusual electronic phenomena and structural features in molecular electronic materials and photosynthetic proteins</b> Philip Lukins.....	930-937
<b>Scanning near-field optical microscopy with white-light illumination: nanoscale imaging and spectroscopy of resonant systems.</b> J.-S. Bouillard and A. V. Zayats.....	938-945
<b>Microscopy in Nanotechnology</b> Shalini Charurvedi and Pragnesh N Dave.....	946-952
<b>Variable Phase- and Bright-Darkfield Contrast – new Illumination Techniques for Advanced Imaging in Light Microscopy</b> T. Piper, and J. Piper.....	953-961
<b>The analysis of hyperspectral broadband coherent anti-Stokes Raman scattering (CARS) microscopic images</b> Alexander Khmaladze.....	962-969

## Educational materials on Microscopy

---

<b>Encouraging scientific cooperation and inclusion through microscopy: a case study</b> G. M. F. V. AQUIJE, A. M. N. KORRES and S. Q. M. LEITE.....	973-976
<b>Introduction to electron microscopy – university educational programme for secondary schools</b> Eliza Rybska, Jerzy Błoszyk and Zbigniew Adamski.....	977-981
<b>Reproductive Biology Research in <i>Cucurbitaceae</i> by High School Students</b> A. Zienkiewicz, A. J. Castro, K. Zienkiewicz, D. G. Caracuel, A. M. Cogolludo, C. Enríquez, J. C. Morales, I. Ruiz-Gámez, M. V. Ruiz-Maldonado, S. Torreblanca, G. Vicente and J. D. Alché.....	982-987
<b>Teaching biology through remote access microscopy</b> G. Nagy, G. Pinczes, P. Papai, G. Kiraly and G. Banfalvi.....	988-993
<b>Teaching Digital Histology</b> Carlos R. Morales.....	994-998
<b>The world we can see - a mirror of the microworld?</b> Eliza Rybska, Zbigniew Adamski, Antoni Wójcik and Jerzy Błoszyk .....	999-1003

## Applications in Physical/Chemical Sciences

---

<b>Brewster Angle Microscopy (BAM) for in situ characterization of ultrathin films at air/liquid interfaces</b> J. J. Giner-Casares and G. Brezesinski.....	1007-1012
<b>Thermomicroscopy and its pharmaceuticals applications</b> R. Chadha, P. Arora, S. Bhandari and M. Bala.....	1013-1024

<b>hermooptical microscopy (TOM) for the investigation of the crystallisation, melting and supermolecular structure of polypropylene and their multicomponent systems</b> József Varga and Alfréd Menyhárd.....	1025-1035
<b>Application of Raman microscopy for spin-phonon coupling and magnon excitation study in nanocrystals</b> Sheng Yun Wu.....	1036-1043
<b>Scanning electron microscopy study of carbon induced corrosion of fired refractory castable</b> P. Ptáček, F. Šoukal, T. Opravil, J. Wasserbauer, J. Havlica and J. Brandštetr.....	1044-1051
<b>The application of high-resolution scanning electron microscopy to inorganic materials</b> Y. Zeng, W. Wu, Z.W. Liu, J.J. Hua, C.C. Lin, Q. Feng.....	1052-1059
<b>FIB-SEM Combination Technique for Characterization of Polymer Composites</b> O. Olea-Mejía, O. Olea-Cardoso and R. Lopez-Castañares.....	1060-1065
<b>Coupling of SEM-EDX and FTIR-ATR to (quantitatively) investigate organic fouling on porous organic composite membranes</b> M Rabiller-Baudry, F. Gouttefangeas, J. Le Lannic and P. Rabiller.....	1066-1076
<b>Using SEM in monitoring changes in archaeological wood: A review</b> Safa A. M. Hamed, Mona F. Ali, Nesrin M. N. El Hadidi.....	1077-1084
<b>Using SEM/EDS for characterization of clay ceramic bearing sugarcane bagasse ash waste</b> K. C. P. Faria and J. N. F. Holanda.....	1085-1092
<b>Relationship between microscopy contributions and durability of cement-based composites</b> Wei-Ting Lin and An Cheng.....	1093-1104
<b>A Review of Scanning Electron Microscopy Investigations in Tellurite Glass Systems</b> Ali Erçin Ersundu, Miray Çelikbilek and Süheyla Aydın.....	1105-1114
<b>Electron Microscopy for the evaluation of concrete surfaces modified by gamma radiation</b> L.I. Avila-Córdoba, G. Martínez-Barrera, F. Ureña-Nuñez and C.E. Barrera-Díaz.....	1115-1122
<b>Influence of irradiated polymeric fibers on the mechanical properties of concretes: analysis by microscopy</b> C. Menchaca-Campos, C.E. Barrera-Díaz, G. Martínez-Barrera and O. Gencel.....	1123-1129
<b>Microscopic study of cotton fibre subjected to different functional treatments</b> C.W. Kan, Y.L. Lam and C.W.M. Yuen.....	1130-1136
<b>Scanning Electron Microscopy (SEM) and Energy Dispersive X-Ray analysis (EDX) of Daughter Minerals in Fluid Inclusions in Layered Silicate Materials</b> A. Ruiz-Conde, E. Garzón and P.J. Sánchez-Soto.....	1137-1145
<b>Morphological characterization of Zn-Based Nanostructured Thin Films</b> A. Gomes, T. Frade and Isabel D. Nogueira.....	1146-1153
<b>Controlled formation of spheres by phase segregation in hybrid organic-inorganic PMMA–SiO<sub>2</sub> systems through the silane coupling agent GLYMOS</b> J. J. Pérez Bueno and D. Morales Acosta.....	1154-1162
<b>Effect of hydrothermal conditions on the morphology and photoluminescence properties of PbMoO<sub>4</sub> powders</b> M.R.D. Bomio, L.S. Cavalcante, R.L. Tranquilin, F.V. Motta, C.A. Paskocimas, M.S. Li, J.A. Varela and E. Longo.....	1163-1170

<b>Scanning electron microscopy analysis of sulfur-polymer composite subjected to induced destruction</b> Milica M. Vlahović and Predrag B. Jovanić.....	1171-1182
<b>Microscopic study of polyethylene terephthalate metallisation</b> W.C. Li, C.L. Mak, C.W. Kan and C.Y. Hui.....	1183-1189
<b>High-resolution (scanning) transmission electron microscopy and related techniques for structural analysis of transition metal oxide nanowires</b> X. H. Zhu.....	1190-1203
<b>Analysis of the WO<sub>3</sub> nanorods growth on mica muscovite by transmission electron microscopy</b> V. Potin, S. Bruyère, M. Gillet and S. Bourgeois.....	1204-1212
<b>Investigation of the elementary mechanisms controlling dislocation/twin boundary interactions in fcc metals and alloys: from conventional to advanced TEM characterization</b> H. Idrissi and D. Schryvers.....	1213-1224
<b>Observation by transmission electron microscopy of organic nano-tubular architectures</b> Noriyuki Ishii.....	1225-1233
<b>Nanostructural characterization of oxide and solid clusters by high-resolution electron microscopy with residual indices</b> Takeo Oku.....	1234-1245
<b>Analytical electron microscopy of gold nanoparticles on nano/microdiamond supports</b> Sónia A.C. Carabineiro, Miguel Avalos-Borja and Josephus G. Buijnsters.....	1246-1251
<b>Analytical TEM/STEM Characterization of Mutual Diffusions Occurred at the Electrolyte-Electrode Interfaces in the Intermediate Temperature Solid Oxide Fuel Cells</b> Zhi-Peng LI, Toshiyuki MORI, Jin ZOU, and John DRENNAN.....	1252-1258
<b>Characterization of nanostructured calcium phosphate-based bioceramics: TEM and SEM/FE-SEM studies</b> Bahman Nasiri-Tabrizi, Abbas Fahami and Reza Ebrahimi-Kahrizsangi.....	1259-1270
<b>Applications of High Resolution Electron Microscopy in Structural Analysis of Nanoarrays</b> Chaolun Liang, Wenxia Zhao, Xianfeng Yang, Mingmei Wu and Yexiang Tong.....	1271-1282
<b>Microscopy as a tool to control predicted morphology and/or dispersion of a binary and ternary compounds in polymeric particles and fibre.</b> A. Cayla and F. Salaün.....	1283-1290
<b>Microscopy Methods in Nanochemistry</b> Alireza Aslani.....	1291-1311
<b>Electron Microscopic Studies on the Lithium Ion Conducting Materials</b> Rajesh Cheruku, Lakshmi Vijayan and G.Govindaraj.....	1312-1323
<b>Photochromism of Ti(III,IV)/PMMA Opalescent Coatings</b> Ll. M. Flores Tandy, J. J. Perez Bueno and Y. Meas Vong.....	1324-1330
<b>Microscopic analysis of bentonite used for adsorption of lead ions in water</b> E. Manriquez Reza, J. J. Perez Bueno and A. Hurtado Macías.....	1331-1336
<b>Atomic Force Microscopy-Based Molecular Recognition: A Promising Alternative to Environmental Contaminants Detection</b> D. K. Deda, C. C. Bueno, G. A. Ribeiro, A. S. Moraes, P. S. Garcia, B. Brito, F. L. Leite.....	1337-1348

<b>Qualitative investigation of the surface electrical potential in ZnO thin films by scanning surface potential microscopy</b> N. S. Ferreira.....	1349-1352
<b>3D-AFM Mapping Surface Investigations and Micro-Structural Surface Features of Some Inorganic Materials</b> Khaled M. Elsabawy.....	1353-1361
<b>Piezoelectric Force Microscopy Study of Domain Structure In High Tc Ferroelectric Films</b> Jingzhong Xiao.....	1362-1369
<b>Thin films from different materials obtained by the Sol-Gel method: study of the morphology through Atomic Force Microscopy (AFM)</b> M. R. Alfaro Cruz , G. Ortega Zarzoza, G. A. Martínez Castañón and J. R. Martínez.....	1370-1376
<b>Scanning Probe Microscopy Investigation of Metal Oxides Nanocrystalline</b> Mingkui Wang, Getachew Alemu and Yan shen.....	1377-1386
<b>Effects of Solvent on Fabrication of Xylan Sulfate Self-Assembled Films Visualized by Atomic Force Microscopy</b> Hao Liu, Heli Cheng, Shicheng Chen, Chaoying Fu, Shiyu Fu and Huaiyu Zhan.....	1387-1394
<b>Nanofriction study using atomic force microscopy (AFM) of multilayers based in titanium, chromium and aluminum</b> L. Ipaz, A. Esguerra-Arce, W. Aperador, F. Espinoza, H. Ruiz.....	1395-1403
<b>Atomic Force Microscopy study on surface of Thai decorative glasses</b> P. Dararutana, K. Won-in, S. Satitkune, U. Tippawan and S. Intarasiri.....	1404-1406
<b>Progress in Scanning Electrochemical Microscopy by Coupling Potentiometric and Amperometric Measurement Modes</b> R. M. Souto, J. Izquierdo, J. J. Santana, A. Kiss, L. Nagy and G. Nagy.....	1407-1415
<b>Deposition and Characterization of Semiconducting Molecular-Material Thin Films by Atomic Force Microscopy and Scanning Electron Microscopy</b> M. E. Sánchez-Vergara, C. Álvarez-Toledano, A. Garduño, J. R. Alvarez-Bada.....	1416-1423
<b>Characterization of nanocomposite coatings on textiles: a brief review on Microscopic technology</b> Mazeyar Parvinzadeh Gashti, Farbod Alimohammadi, Guowen Song, Amir Kiumarsi.....	1424-1437
<b>A comparison of atomic force microscopy, confocal fluorescence microscopy and Brewster angle microscopy for characterizing mixed monolayer surfactant films.</b> Ala'a F. Eftaiha, Sophie M.K. Brunet and Matthew F. Paige.....	1438-1447
<b>Complementary microscopy techniques for surface characterisation of uncoated and mineral pigment coated paper</b> Gary Chinga-Carrasco.....	1448-1455
<b>Microscopy tools for investigating nano-to-mesoscale peptide assemblies</b> Emerson R. da Silva, Michelle S. Liberato, Márcia I. de Souza, Rondes F. da Silva, Iorquirene O. Matos, Sérgio Kogikoski Jr., Roberta C. Bianchi and Wendel A. Alves.....	1456-1467
<b>Development of Nano-Structured HTSC for Application in Medicine</b> M. Muralidhar, M R. Koblischka and M. Tomita.....	1468-1479
<b>Microscopic and microanalytical examinations of metallic particles and single textile fibres for forensic purposes</b> Z. Brozek-Mucha and J. Was-Gubała.....	1480-1491

<b>Entropy-Enthalpy Compensation: Is there an Underlying Microscopic Mechanism?</b> E. B. Stariko, and B. Nordén.....	1492-1503
<b>Synchrotron soft x-ray and infrared microspectroscopy contributions to advances in feed chemistry and feed science technology</b> Peiqiang Yu.....	1504-1510
<b>Automatic microscopes for nuclear emulsion readout in high-energy and particle physics</b> C. Bozza , T. Nakano.....	1511-1523

## Electron Microscopy for the evaluation of concrete surfaces modified by gamma radiation

L.I. Avila-Córdoba<sup>1</sup>, G. Martínez-Barrera<sup>2</sup>, F. Ureña-Nuñez<sup>3</sup> and C.E. Barrera-Díaz<sup>1</sup>

<sup>1</sup>Centro Conjunto de Investigación en Química Sustentable (CCIQS), Universidad Autónoma del Estado de México – Universidad Nacional Autónoma de México (UAEM-UNAM), Carretera Toluca-Atlaconulco, km 14.5, Unidad El Rosedal, C.P. 50200, Toluca México.

<sup>2</sup>Laboratorio de Investigación y Desarrollo de Materiales Avanzados (LIDMA), Facultad de Química, Universidad Autónoma del Estado de México, Km. 12 de la carretera Toluca-Atlaconulco, San Cayetano 50200, México.

<sup>3</sup>Instituto Nacional de Investigaciones Nucleares, Carretera México-Toluca S/N, La Marquesa Ocoyoacac 52750, México.

As we know the electron microscopy has shown its effectiveness as tool for surfaces analysis. Depending on the material is possible to describe surface features as roughness, smoothness, and so. In the case of composite materials is essential the analysis of the contributions of each component of the composite. For the case of concrete or mortar materials, some approaches have been developed and general statements are taken as standard parameters. The hydraulic concrete derived from a mixture of cement, rough and fine aggregates and water. Each one contributes on the final features of concrete, including the mechanical properties. The morphology of each component takes into account size, shape, roughness, etc. In this chapter we discuss the importance of the electron microscopy for to describe the influence of the components after mechanical testing, and some predictions can be planned for to avoid fractures.

**Keywords:** scanning electron microscopy; hydraulic concrete; polymer concrete; gamma radiation.

### 1. Introduction

Ordinary Portland Cement Concrete (PCC) is one of the oldest man-made materials and is important among inorganic building materials. The success of PCC as a building material derives mainly from its inexpensive cost and many desirable properties. The use of Portland cement, however, is not limited to construction of buildings but may also be used, as an example, for waste immobilization. The components of PCC are well known: rocks and/or gravel (coarse aggregate), sand (fine aggregate), hydrated Portland cement, and usually voids – with the coarse aggregate making up the majority of the concrete and the hydrated Portland cement binding the whole material.

Development of another alternative to PCC was begun in the 1960s with the incorporation of organic polymers into cement concrete, giving a new class of composite building materials. Since that time, knowledge of so-called Polymer Concrete (PC) has significantly progressed. Polymer concrete is a composite material formed by combining mineral aggregates (such as sand or gravel) with a monomer, usually of a thermoset polymer resin. To form the final concrete product, the monomer must be cured, forming a network of polymer chains from the original monomeric compound. Therefore in PC we have a polymeric matrix as the continuous phase and dispersed inorganic particles as a discrete phase [1].

Typically PC has a longer maintenance-free service life than PCC and possesses also other advantages compared to PCC such as: increased bond strength (bonding to previously existing concrete); increased freeze-thaw resistance; high abrasion resistance; increased flexural, compressive and tensile strengths; fast setting times (curing within 1 or 2 h); good durability; improved chemical resistance in harsh environments [2, 3]. Moreover, they exhibit good creep resistance [4], and are highly UV resistant due to the very low polymer content and inert fillers. On the other hand, they exhibit reduced elastic modulus. The loss of strength can be attributed to an increase of porosity in PCs with increased capillary diffusion of solutions, which weakens the bond between the aggregate and the matrix [5].

### 2. Portland Cement Concrete after gamma irradiation

In the case of hydraulic concrete (PCC), some modifications on the cement and silica sand have been done by using gamma radiation; such materials are mixing into the concrete. In other case all concrete components are mixed and then the concrete specimens are irradiated. Both kinds of concretes are evaluated by mechanical tests. The results are different, and the scanning electron microscopy has been a good tool for to evaluate the contribution of each component in non-irradiated and irradiated concretes.

For the morphological characterization, after mechanical testing, some fractured hydraulic concrete pieces were dried in a rotovapor for 24 hours. After, they are vacuum-coated with carbon (coating thickness between 3 to 10 nm) in a vacuum pump at 50 mTorr. Then the surfaces of fractured zones are analyzed by scanning electron microscopy (SEM) in the secondary electron mode, which provides good images of distribution of dispersed phases in a matrix [6 - 10].

Moreover, the surfaces of silica sand and marble, before and after irradiation were analyzed following the specifications as fracture concrete samples. The secondary electron mode is preferred in the present case, because provided good contrast between the constituents. While for instance in characterization of polymer + metal hybrids micro powder, backscattered electrons provide a better contrast [7, 11].

Surface modifications of silica sand are shown in Figure 1. Evident is deterioration of silica sand surfaces with increasing irradiation. For non-irradiated silica sand a homogeneous surface is seen, with a few cracks  $\approx 5 \mu\text{m}$  long (Figure 1a); when increasing the radiation dose, several particles smaller than  $5 \mu\text{m}$  in average size appear (Figure 1b); and finally for the high dose of 150 kGy deteriorated surface with several cracks (Figure 1c) is seen. The mechanical performance of the concrete can be related to morphological changes on the surfaces. Moreover, some conclusions can be done after analyzing surfaces of the concrete components after submitted to gamma radiation. For example, the cracks propagating on surfaces of silica sand particles can relate with the lower compressive strength values obtained at higher gamma dosages.

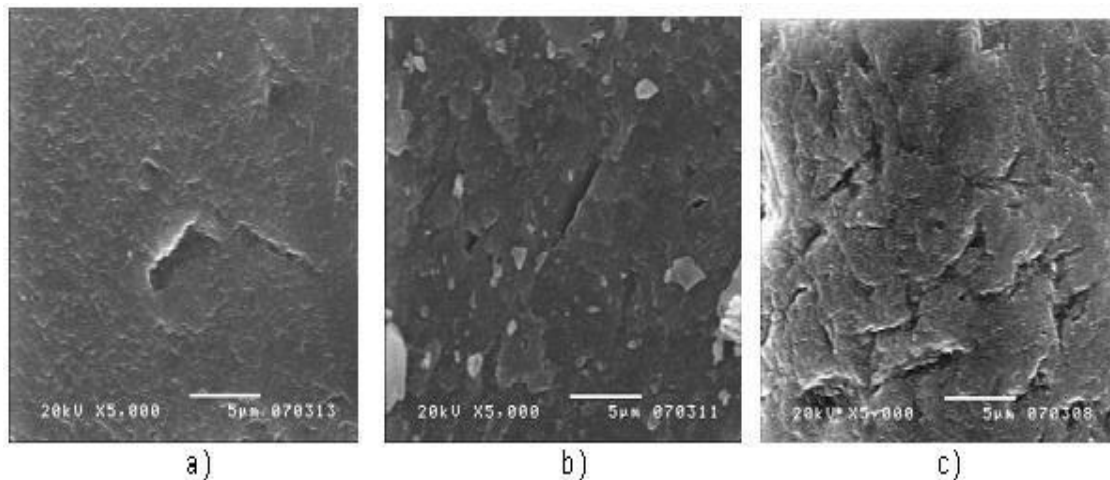


**Fig. 1** SEM images of silica sand: a) non-irradiated, b) irradiated at 50 kGy, and c) irradiated at 150 kGy.

A literature survey shows that relatively little attention has been paid to the morphology of silica sand and its contribution to mechanical improvement of concrete. Evident in Figure 2 are morphological changes dependent on the irradiation dose. Crazes and some grooves are observed. The number of the crazes increases with the irradiation dose; the crazes are well developed at 150 kGy, about  $100 \mu\text{m}$  long and a certain “branching” tendency is seen. The wrinkles have more contact points – thus providing stronger adherence of sand to the hydrated cement. Herein lay an explanation of the property improvement resulting from irradiation [8].

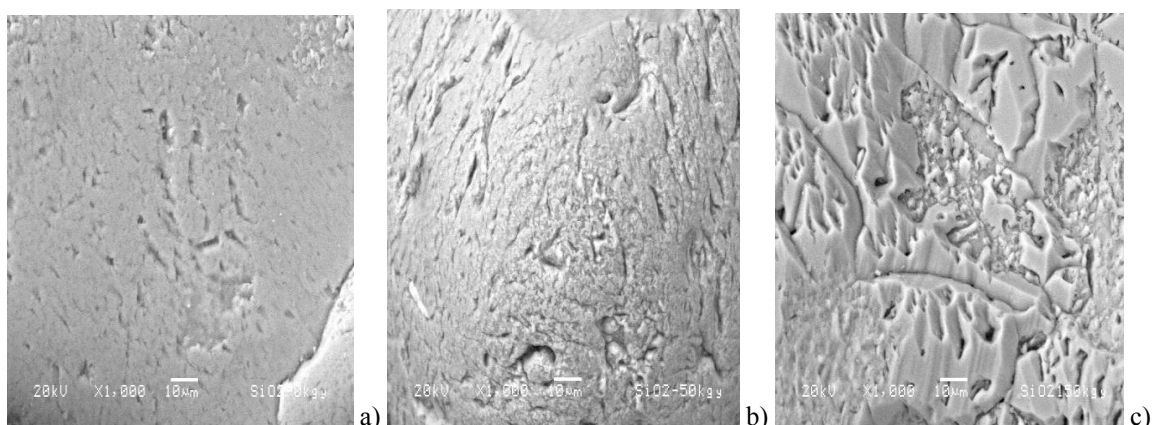


**Fig. 2** SEM images of silica sand: a) non-irradiated, b) irradiated at 50 kGy, and c) irradiated at 150 kGy.

We see in Figure 3 that the marble morphology exhibits similar behavior to the silica sand. That is, for non-irradiated marble, several particles are seen (Figure 3a); after increasing the gamma radiation dose to 50 kGy, more particles with larger sizes appear (Figure 3b). For the high dose of 150 kGy, the particle size is still larger due to degradation of the marble (Figure 3c). As noted previously, mechanical performance of the concrete can be related to morphological changes on the surfaces. In some cases the dynamic elasticity modulus  $E_d$  values of concretes are lower than those for non-irradiated, thus a more ductile concrete is formed - pertinent in the case of seismic events [9].



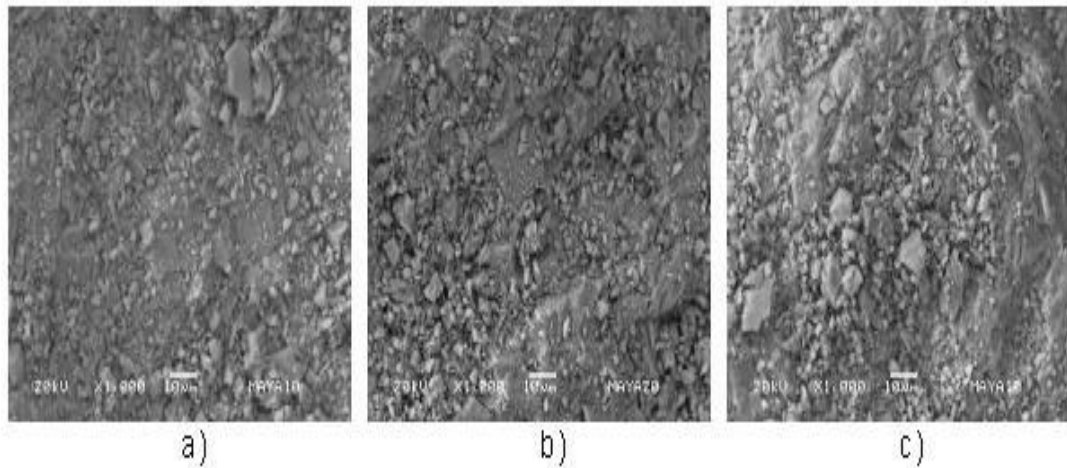


**Fig. 3** SEM images of marble: a) non-irradiated, b) irradiated at 50 kGy, and c) irradiated at 150 kGy.

Concretes consisting of Portland cement, silica sand, marble and sludge were developed. The sludge was subjected to two series of treatments. In one series, coagulants were used, and in the other series, an electrochemical treatment was applied with several starting values of pH. The compressive strength, compressive strain at yield point, and static and dynamic elastic moduli were determined [12]. The sludge generated by the electrochemical process at pH = 7 and the fractured concrete specimens were analyzed by scanning electron microscopy (SEM) and energy dispersive X-ray microanalysis (EDS). The sludge shows a heterogeneous morphology, as shown in Fig. 4a. Its elemental composition as determined by EDS includes carbon (20.9 %), oxygen (46.9%), iron (16.2%), and sodium (2.2%) as the main elements (Fig. 4b).

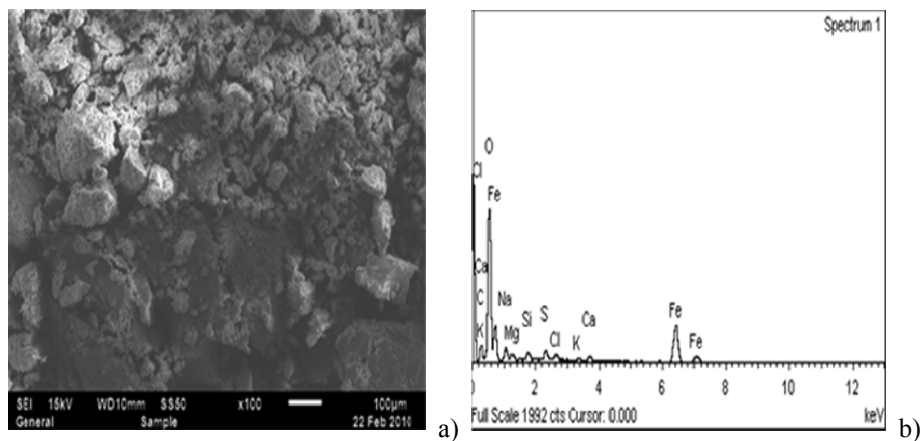


**Fig. 4** a) SEM image of dry sludge, and b) Microanalysis image (EDS) of dry sludge.

Figure 5 shows the morphology of the fractured surfaces of the concretes (seven days curing) subject to compressive testing. For the concrete with higher silica sand content, the surface of the sludge containing material (Fig. 5b) is less rough than the specimen without sludge (Fig. 5a). The sludge seems to act as a wrapper for the marble particles. For the concrete with lower silica sand content, both surfaces are fairly similar (Figs. 5c and 5d). Somewhat larger marble particles are seen in the absence of sludge. From Figure 5d, it is inferred that the amount of sludge is insufficient to cover all silica sand particles. The presence of sludge has beneficial effects on the long term properties and for to improve the compressive strain at yield point of concrete.

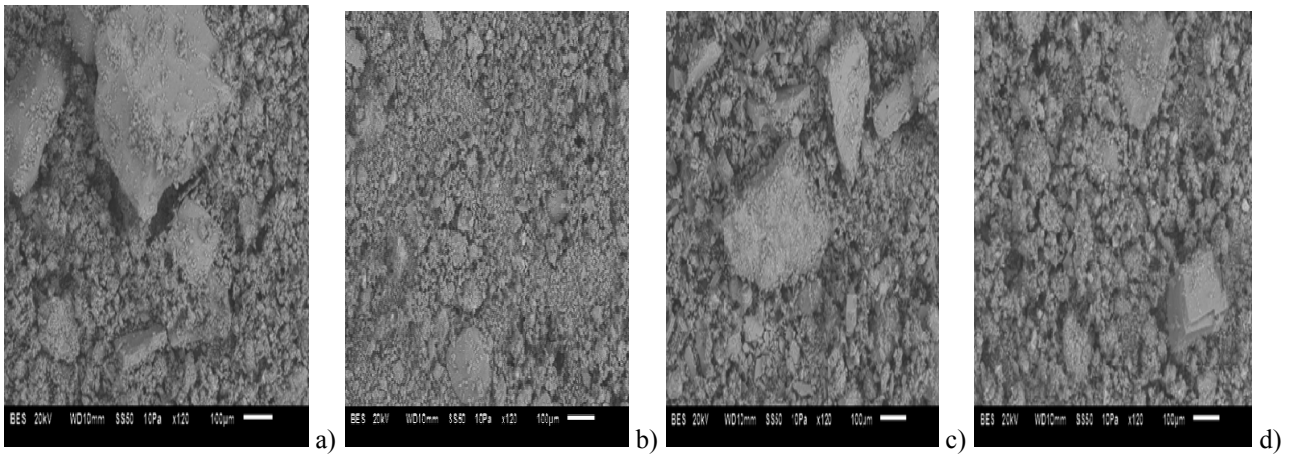


**Fig. 5** SEM images of the curing concrete (at 7 days) after compressive testing: a) Higher silica content, b) Higher silica content and sludge, c) Lower silica content, and d) Lower silica content and sludge.

### 3. Polymer Concrete after gamma irradiation

As we remind, polymer concrete is a composite material formed by combining mineral aggregates (such as sand, marble,  $\text{CaCO}_3$  or gravel) with a monomer, usually of a thermoset polymer resin. To understand the changes of the elasticity modulus of the polymer concrete, the neat polyester resin is irradiated and studied the morphological changes by SEM (Figure 6). For non-irradiated resin, a homogeneous surface is seen. It contains regions not fully polymerized by the MEKP catalyst (Figure 6a). When applying 50 kGy of irradiation (Figure 6b), a surface consists of several constraining regions, apparently responsible for the elasticity modulus. At 100 kGy, the gamma radiation results in the presence of two morphologies on the resin surface, constrained regions, and voids, what leads to the highest elasticity modulus (Figure 6c).

Improvement in mechanical properties caused by irradiation is clearly related to morphology of the components and the void volume in the composites. The larger the irradiation dose, the larger are the void volumes, caused by morphology deteriorations suffered by the polyester resin. An adequate aggregate gradation can provide low void volumes and thus good mechanical strength. Variations in the gamma radiation dose enable modification of the void volume and thus higher compressive strain [11].

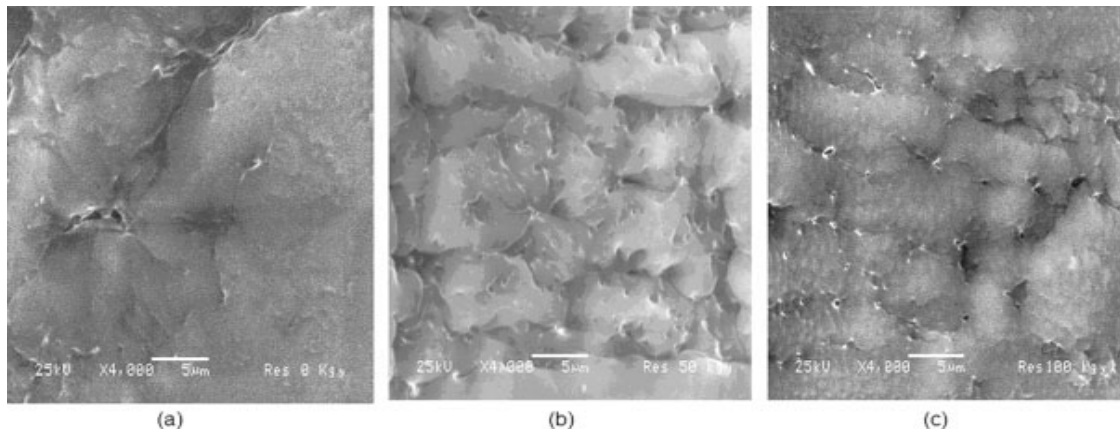


**Fig. 6** SEM images of polyester resin: a) non-irradiated, b) irradiated at 50 kGy, c) irradiated a 100 kGy.

The high compressive strain values can be explained in terms of surface morphology of the polymer concrete. For irradiated polymer concrete at 5 kGy, a heterogeneous morphology is observed, including the aggregate particles covered by polyester resin (Figure 7a). When increasing the applied radiation dose, a softer surface is seen and the aggregate particles are fully covered (Figure 7b). This situation is a consequence of crosslinking of the chains in the polyester resin. Moreover, for higher applied doses, the polyester resin is constrained, the surfaces show more agglomeration regions, what produces the highest compressive strain values (Figure 7c). In the 0–50 kGy interval, there is chain reorientation due to the polymerization in the polyester resin with an increase in the crystallinity; however, if the radiation process goes on, the damage can be permanent. The lowest compressive strain value is at 10 kGy, what implies there is an influence of the polyester resin.

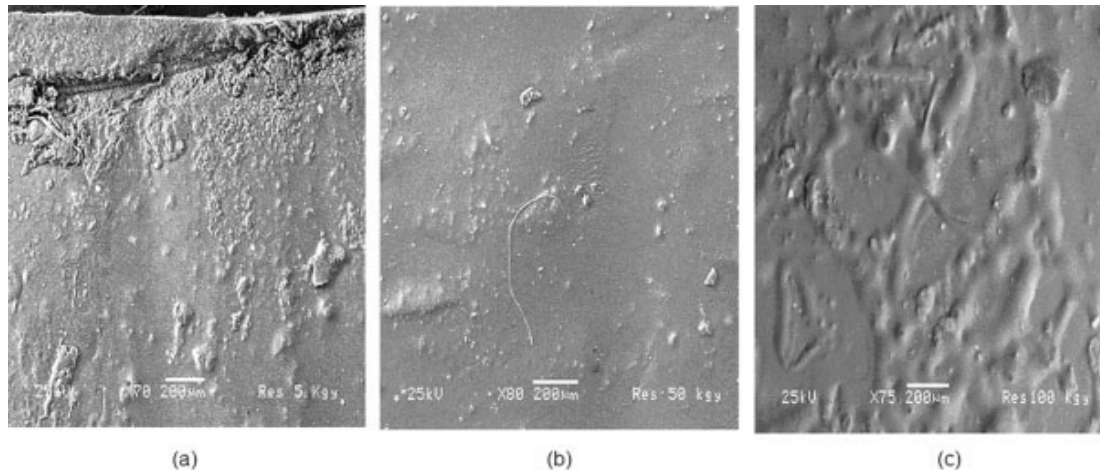


**Fig. 7** SEM images of polymer concrete irradiated at: a) 5 kGy, b) 50 kGy, and c) 100 kGy.

The compressive strain values can be related to the morphology of the polymer concrete surfaces fractured after testing. For polymer concrete irradiated at several doses and elaborate with two different sizes of the marble particles. The compressive strain values for 5 and 10 kGy are the same, but lower by 29% at 50 kGy. At low doses the marble particles are covered by the polyester resin; several scrap particles (produced by the compression force) smaller than 10  $\mu\text{m}$  are seen (Figures 8a and 8b). When increasing the applied radiation dose, a larger number of scrap particles and cracks passing through the marble particles are seen (Figure 8c). A large number of such cracks provide more ductile concrete. The cracks are a consequence of the polyester constraints resulting from crosslinking of the chains in the polyester resin.

The compressive strain behavior of polymer concretes with three-particle sizes, has three stages: a) a decrease from non-irradiated to 10 kGy; b) an increase up to 50 kGy; and c) a decrease at higher doses (100 and 150 kGy). Thus, the combination of three different particle sizes results in a harder material. Compressive strain values are lower than those for polymer concretes with two particles sizes. Then combination of two or three different particle sizes into the concrete generate a harder material - instead of a ductile material created when only one particle size is used [10].

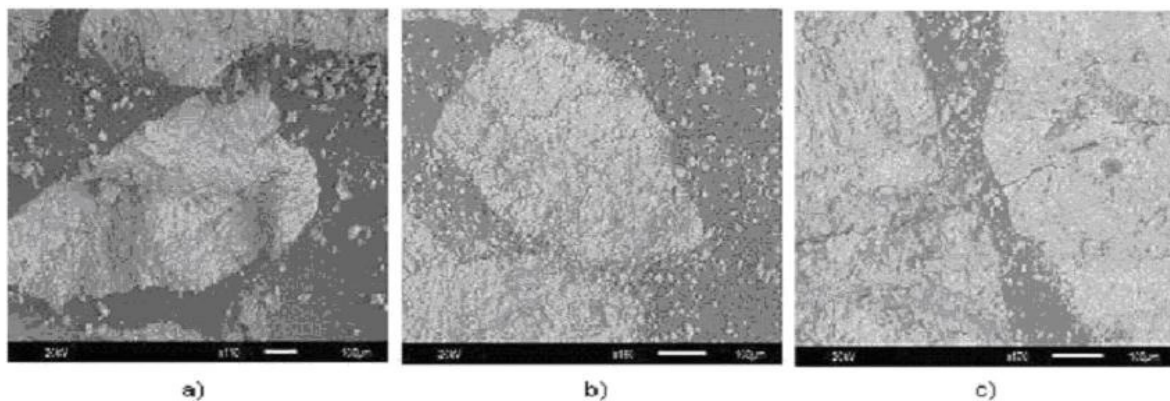


**Fig. 8** SEM images of polymer concrete irradiated at: a) 5 kGy, b) 10 kGy, and c) 50 kGy.

The morphological modifications of marble after irradiation are related with mechanical properties of the concrete. Homogeneous surfaces on marble particles are seen for non-irradiated samples (Figure 9a). When increasing the dose to 100 kGy, scraped particles are generated (Figure 9b), and for a dose of 150 kGy a partial destruction of the marble particles (Figure 9c). Gradual deteriorate on the marble particles when increasing the applied dose, and thus gradual lowering of the compressive strength [13].

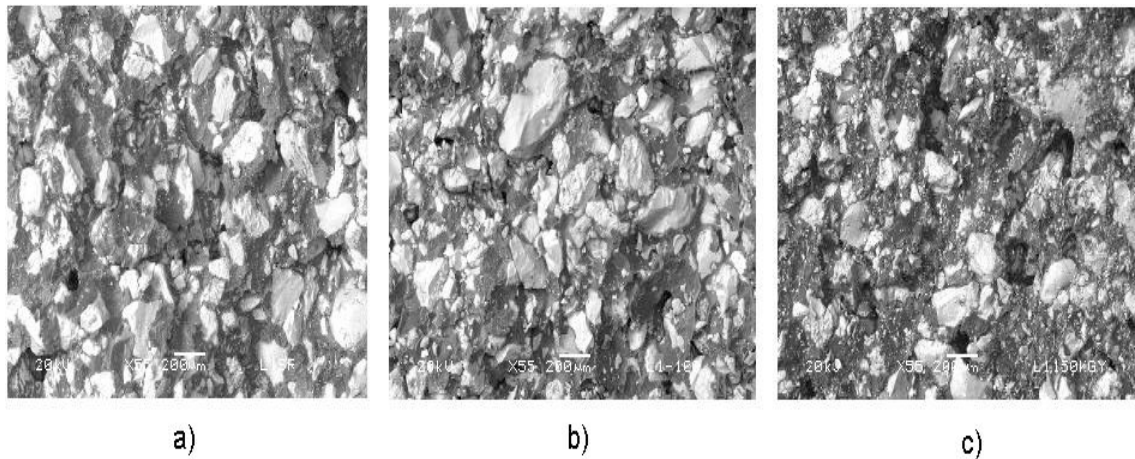


**Fig. 9** SEM images of fractured zones of concretes: a) non-irradiated, b) irradiated at 100 kGy, and c) irradiated at 150 kGy.

In Fig. 10 we show the fracture zone after testing the polymer concrete with 38% of resin and 62% of silica sand. For non-irradiated PC an analysis of silica sand and polyester resin was carried out (Fig. 10a). First, sand particles are well visible with sizes below 50  $\mu\text{m}$ , contributing to the material resistance against deformation under a compressive load. Then, the particles tend to disintegrate; the original particles had the diameters of 150  $\mu\text{m}$  on the average. The resin has a homogeneous surface and totally covers the sand particles [7].

When increasing the irradiation dose, the mechanical features are improved. However, for the high level radiation, namely 100 kGy, the mechanical parameters decrease. In the SEM image corresponding to 100 kGy (Fig. 10b), we observe less disaggregate sand particles whose sizes are not smaller than non-irradiated PC. Moreover, crack formation in the resin is seen, thus, a separation between the sand particles and the resin occurs. This causes lowering of both the compressive strength and strain values. On the other hand, we get high elastic modulus. At the highest radiation dose of 150 kGy, an evident separation between resin and the particles is seen. Some small particles, with the diameter below 50  $\mu\text{m}$  on the average, are observed (Fig. 10c). In principle, when the PC has more space between resin and the particles (caused by gamma radiation), the elastic modulus increases but the compressive strength decreases.

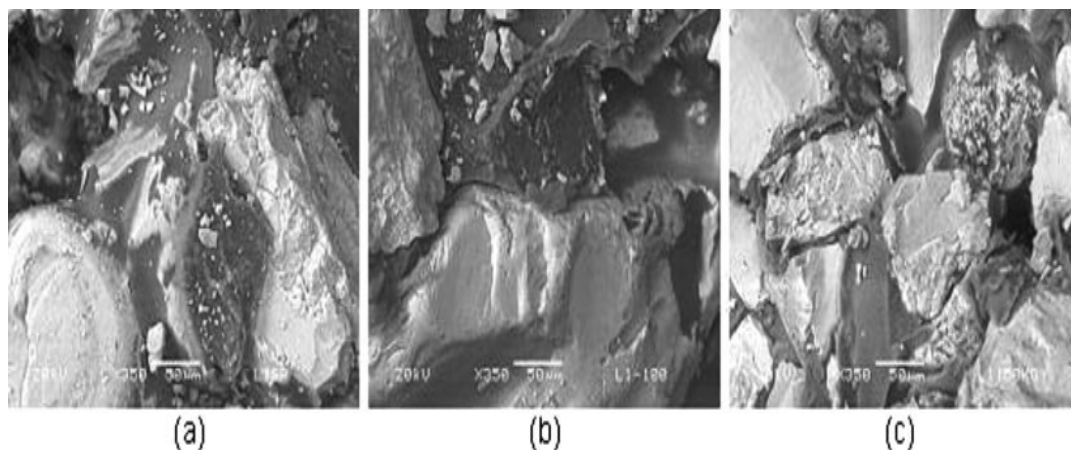


**Fig. 10** SEM images of polymer concrete after compressive test: a) non-irradiated, (b) irradiated at 100 kGy, and c) irradiated at 150 kGy.

Moreover, the morphology of the non-irradiated resin shows a homogeneous surface (Figure 11a). For higher doses striations are seen, apparently a consequence of the resin contraction (Figure 11b). We emphasize that the resin provides major contributions to the mechanical improvement of the concrete. Then, if a sand particle is present in a non-irradiated resin matrix, it will be surrounded by the resin. When the radiation has been applied, the resin will start its polymerization, what will cause the following effects: breakdown of the resin (cracks) and resin contraction with pulling out from the sand particles. As already reported by Ismail et al., the interaction between cement constituents and polyester formed in the pores under the effect of gamma irradiation contribute to an improvement in the mechanical strength [14].

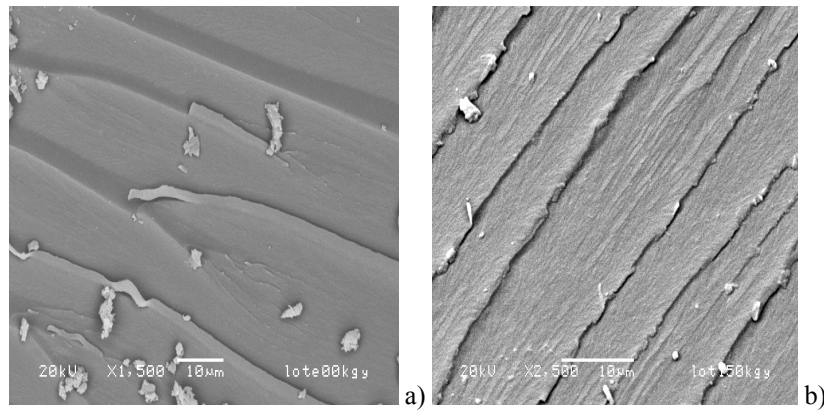


**Fig. 11** SEM images of the polyester resin: a) non-irradiated, b) irradiated at 150 kGy.

The surfaces of the fractured zone of the manufactured polymer concrete, before and after irradiation, were analyzed by scanning electron microscopy. The concretes were elaborated with insaturated polyester resin and  $\text{CaCO}_3$  particles. For the concrete irradiated at 10 kGy, when adding more solid  $\text{CaCO}_3$  particles (Figure 12a), strong interactions appear, resulting in a hard material. As a consequence, significant restrictions on molecular mobility of the polyester resin around the  $\text{CaCO}_3$  particles occur and an increment of the stiffness results. This does not happen when the samples contain less  $\text{CaCO}_3$  particles (Figure 12b), weak interfacial interactions are present and the elastic modulus diminishes.

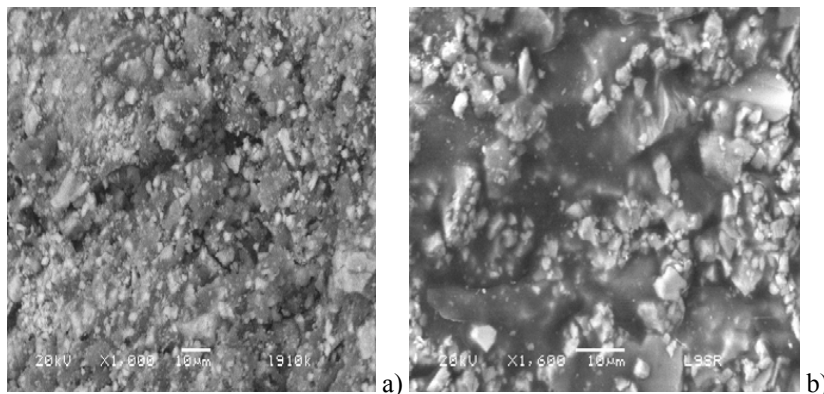


**Fig. 12** SEM images of irradiated polymer concrete at 10 kGy, with: a) 46 % of the resin, b) 60 % of the resin.

It was suggested by the Zagreb group that the degree of the reinforcement of the composites may be a result of interdiffusion and entanglements between the homopolymer and polymer molecules grafted on the  $\text{CaCO}_3$  surface and the polymer matrix molecules [15].

For samples irradiated up to 10 kGy both compressive strain and compressive modulus of elasticity increase; we can presume that the polymerization of the resin still is not complete; more polymerization can be achieved by the irradiation energy input as discussed by Saiter and collaborators [16]. The Rouen group points out that two post-curing processes are necessary. With these treatments it is possible to get  $\approx 95\%$  of total polymerization. In our case, by means of applied radiation it is possible to obtain lower compressive strain but an increase of the compressive modulus of elasticity. Moreover, the effects of the radiation up to 10 kGy allow formulating the following rule: higher concentrations of the resins results in higher values of the compressive modulus of elasticity.

According to the electron microscopy analysis, changes in the mechanical properties are related to the distribution of the  $\text{CaCO}_3$  particles in the polyester resin and the adhesion between them. We emphasize that the resin provides major contributions to the mechanical improvement of the concrete. Differences in mechanical properties are significant when comparing to the non-irradiated resin: 223% for compressive strength, 66% for the compressive strain, and 105% for the compressive modulus of elasticity.

**Acknowledgements.** Mr. Miguel Martínez López and Ms. Elisa Martínez Cruz graduated students at the Materials Science Program (UAEM) have participated in the experiments. CONACYT grant 153828.

## References

- [1] Martínez-Barrera G, Viguera-Santiago E, Gencel O, Hagg Lobland HE. Polymer concretes: a description and methods for modification and improvement, *J. Mater. Ed.* 2011; 33: 37-52.
- [2] Fowler DW. Polymers in concrete: a vision for the 21st century, *Cement & Concrete Composites* 1999; 21: 449-452.
- [3] Vipulanandan C, Paul E. Characterization of polyester polymer and polymer concrete, *Journal of Materials in Civil Engineering* 1993; 5: 62 - 82.
- [4] Reis JML, A comparative assessment of polymer concrete strength after degradation cycles, in *Mechanics of Solids in Brazil 2009*, Brazilian Society of Mechanical Sciences and Engineering, Brazil; 2009.
- [5] Ahn N. Effects of diacrylate monomers on the bond strength of polymer concrete to wet substrates *J. Appl. Polym. Sci.* 2003; 90: 991-100.
- [6] Martínez-Barrera G, Espinosa-Pesqueira ME, Brostow W. Concrete + polyester + CaCO<sub>3</sub>: Mechanics and morphology after gamma irradiation, *e-Polymers* 2007; 83: 1-12
- [7] Martínez-Barrera G, Texcalpa-Villarruel U, Viguera-Santiago E, Hernández-López S, Brostow W. Compressive strength of Gamma-irradiated polymer concrete, *Polym. Compos.* 2008; 29: 1210-1217.
- [8] Martínez-Barrera G, Martínez-Hernández AL, Velasco-Santos C, Brostow W, Polymer concretes improved by fiber reinforcement and gamma irradiation, *e-Polymers* 2009; 103: 1-14.
- [9] Martínez-Barrera G, Menchaca-Campos C, Viguera-Santiago E, Brostow W. Post-irradiation effects on Nylon-fiber reinforced concretes, *e-Polymers* 2010; 42: 1-13.
- [10] Martínez-Barrera G, Brostow W. Effect of marble particle size and gamma irradiation on mechanical properties of polymer concrete, *e-Polymers* 2010; 61: 1 – 14.
- [11] Martínez-Barrera G, Giraldo LF, López BL, Brostow W. Effects of gamma radiation on fiber reinforced polymer concrete, *Polym. Compos.* 2008; 29: 1244-1251.
- [12] Barrera-Díaz C, Martínez-Barrera G, Gencel O, Brostow W, Bernal-Martínez LA. Processed wastewater sludge for improvement of mechanical properties of concretes, *Journal of Hazardous Materials* 2011; 192: 108 – 115.
- [13] Martínez-Barrera G, Ureña-Núñez F, Gencel O, Brostow W. Mechanical properties of polypropylene-fiber reinforced concrete after gamma irradiation, *Composites: Part A* 2011; 42: 567 – 571.
- [14] Ismail MR, Ali MA, EI-Milligy AA, Afifi MS. Physico-chemical studies of gamma-irradiated polyester - impregnated cement mortar composite, *J. Radioanal. Nucl. Chem.*, 1998; 238: 111-117.
- [15] Leskovic M, Kovacevic V, Lucic Blagojevic S, Vrsaljko D, Volovsek V. Pre-treatment of CaCO<sub>3</sub> nanofiller by irradiation in the presence of vinyl monomers for the preparation of poly(vinyl acetate) composites, *e-Polymers* 2004; 33: 1-13
- [16] Delahaye N, Marais S, Saiter JM, Metayer M. Characterization of unsaturated polyester resin cured with styrene, *J. Appl. Polym. Sci.* 1998; 67: 695-703.